Stem Cells Translational Medicine, 2022, **11**, 310–321
https://doi.org/10.1093/stcltm/szab019
Original Research

Alterations in Hematopoietic and Mesenchymal Stromal Cell Components of the Osteopetrotic Bone Marrow Niche

Inci Cevher Zeytin[1,2], Berna Alkan[1,2], Cansu Ozdemir[1], Duygu Uckan Cetinkaya[1,2,3,*], Fatma Visal Okur[1,2,3,*]

[1]Center for Stem Cell Research and Development PEDI-STEM, Hacettepe University, Ankara, Turkey
[2]Department of Stem Cell Sciences, Institute of Health Sciences, Hacettepe University, Ankara, Turkey
[3]Department of Pediatrics, Division of Pediatric Hematology and Bone Marrow Transplantation Unit, Faculty of Medicine, Hacettepe University, Ankara, Turkey

*Corresponding authors: Duygu Uckan Cetinkaya and Fatma Visal Okur, Center for Stem Cell Research and Development (PEDI-STEM), Hacettepe University, Ankara, Turkey, Email: fvokur@hacettepe.edu.tr (F.V.O.), duyguc2008@gmail.com (D.U.C.).

Abstract

Osteopetrosis is a rare inherited disease characterized by impaired osteoclast activity causing defective bone resorption and bone marrow aplasia. It is fatal in early childhood unless hematopoietic stem cell transplantation is performed. But, the transplant course is complicated with engraftment failure. Recently, osteoclasts have been described as the potential regulators of hematopoietic stem cell (HSC) niche. Here we investigated the alterations in the HSC and mesenchymal stromal cell (MSC) components of osteopetrotic niche and their interactions to mimic the stem cell dynamics/trafficking in the BM niche after HSC transplantation. Induced pluripotent stem cells were generated from peripheral blood mononuclear cells of patients with osteopetrosis carrying TCIRG1 mutation. iPSC lines were differentiated into hematopoietic and myeloid progenitors, then into osteoclasts using a step-wise protocol. We first demonstrated a shift toward monocyte-macrophages lineage regarding hematopoietic differentiation potential of osteopetrotic iPSC-derived hematopoietic progenitors (HPCs) and phenotypically normal and functionally defective osteoclast formation. The expression of the genes involved in HSC homing and maintenance (Sdf-1, Jagged-1, Kit-L, and Opn) in osteopetrotic MSCs recovered significantly after coculture with healthy HPCs. Similarly, the restoration of phenotype, impaired differentiation, and migratory potential of osteopetrotic iHPCs were observed upon interaction with healthy MSCs. Our results establish significant alterations in both MSC and HPC compartments of the osteopetrotic niche, and support the impact of functionally impaired osteoclasts in defective niche formation.

Key words: osteopetrosis; TCIRG1; iPSC; hematopoietic niche; hematopoietic progenitors; mesenchymal stromal cells; mesenchymal stem cells.

Graphical Abstract

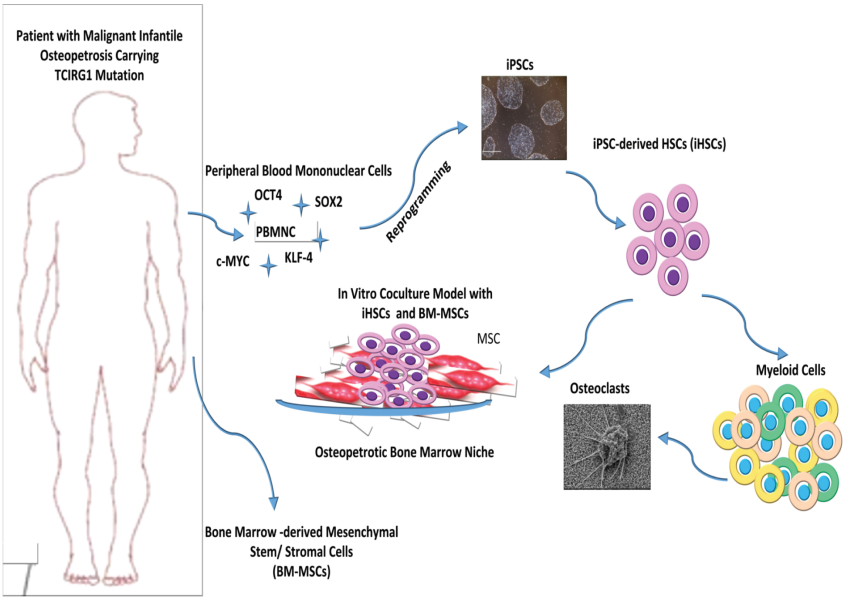

Received: 11 May 2021; Accepted: 7 November 2021.

Significance Statement

Malignant infantile osteopetrosis is a rare genetic disease characterized by the impairment of osteoclast activity resulting in defective bone resorption and progressive bone marrow failure. The only curative treatment is allogeneic bone marrow transplantation providing monocyte-derived donor source of functional osteoclasts. Despite the improvement of transplant strategies and better long-term survival after transplantation, morbidity and mortality rates within the first year after transplantation are still high, with graft failure and early transplant-related complications accounting for most deaths. There is evidence suggesting that the difficulty in achieving engraftment in osteopetrosis is associated with abnormalities in the bone marrow niche and hematopoietic stem cell homing.

Highlights

- Osteopetrotic iPSC-derived hematopoietic progenitors (HPCs) demonstrate a shifted differentiation potential toward monocyte-macrophage lineage.
- Osteopetrotic osteoclasts are phenotypically identical to healthy donor osteoclasts, but functionally defective.
- The regulatory role of osteopetrotic mesenchymal stromal cells (MSCs) in HPC differentiation potential, homing and maintenance in bone marrow is impaired.
- Restoration of MSC activity reestablishes normal HPC phenotype and function, supporting the impact of dysfunctional osteoclast in defective niche formation in osteopetrosis.

Introduction

Osteopetrosis is a rare inherited disease characterized by impaired osteoclast activity causing defective bone resorption and a significant increase in bone mass. Inheritance can be autosomal recessive, dominant, or X-linked, but most severe cases are almost exclusively, autosomal recessive and named as malignant infantile osteopetrosis (MIOP) or autosomal recessive osteopetrosis (ARO). The lack of functional osteoclasts leads to a bone marrow cavity insufficient to support normal hematopoiesis. The resulting extramedullary hematopoiesis gives rise to massive hepatosplenomegaly and macrocephaly. Bony overgrowth results in cranial nerve dysfunction, choanal stenosis, abnormal dentition and developmental delay. Untreated MIOP has a mortality rate of approximately 70% by 6 years of age, mostly due to complications related to bone marrow failure. Mutations in several genes have been implicated in the pathogenesis of osteopetrosis, affecting osteoclast development, differentiation (RANK and RANKL; osteoclast-poor form), and function (TCIRG1, CLCN7, OSTM1, CA-II, and PLEKHM1; osteoclast-rich form).[1-3] Different loss-of-function mutations in T-cell immune regulator 1 (TCIRG1) gene, which encodes vacuolar (V)-ATPase isoform a3, a subunit of the osteoclast vacuolar proton pump, account for almost 50% of all children with infantile osteopetrosis, impair osteoclast ruffled-border formation and bone resorption by disturbing secretory lysosome trafficking.[4] Allogeneic hematopoietic stem cell transplantation (HSCT) is the only curative treatment for most children with osteopetrosis, which needs to be done as early as possible before the development of irreversible neurological complications. Transplantation of hematopoietic progenitor cells is intended to reverse the process by providing monocyte-derived donor source of functional osteoclasts, but bone remodeling and establishment of normal hematopoiesis require time. Despite the improvement of transplant strategies and better long-term survival after transplantation, morbidity and mortality rates within the first year after transplantation are still high, with graft failure and early transplant-related complications accounting for most deaths. There is a definitive need to develop new transplant strategies that will support hematopoiesis to improve engraftment besides providing functional osteoclasts by healthy allografts. There is evidence suggesting that the difficulty in achieving engraftment in osteopetrosis is associated with abnormalities in the bone marrow (BM) niche and hematopoietic stem cell (HSC) homing.[1,5] In a pilot study from our group, we demonstrated that concomitant infusion of BM-derived mesenchymal stromal cells (BM-MSCs) from healthy donors during allogeneic HSCT improved transplant outcomes including achievement of sustained long-term donor engraftment in 11 out of 12 patients with MIOP.[6] Patients with osteopetrosis present with defective bone resorption and hematopoietic alterations, but their bone marrow HSC and osteoclast contents might be different. In patients with osteoclast-rich osteopetrosis there is a significant reduction in HSC pool and fibrosis in bone marrow, whereas the presence of some HSC pool has been reported in patients with osteoclast-poor osteopetrosis.[7,8] There are established experimental models of osteopetrosis in which the osteoclasts and BM niche were studied.[7,9,10] However, animal models are not representative of the human disease and there is paucity of data about the osteopetrotic BM microenvironment in humans. A number of studies have reported alterations in the BM-MSCs of patients with osteopetrosis, including their differentiation potential.[11,12] Investigation of the mechanism of defective osteoclast function and its role in HSC niche formation and maintenance would be critical to understanding altered hematopoiesis in osteopetrosis.

HSCs are maintained in the specialized bone marrow niches in which the fate of HSCs with regard to quiescence, proliferation, differentiation and migration is regulated.[13,14] HSCs reside in the endosteal region, at the interface between the bone and BM, which is the region of active bone remodeling. Enchondral ossification which is essential for the initial formation of HSC niches in bone marrow is tightly controlled by bone modeling/remodeling involving bone-forming osteoblasts and bone-resorbing osteoclasts.[15,16] Although the role of osteoblasts located in the endosteal region of bone is well known in the establishment of BM niches, osteoclasts have been mostly studied in HSC mobilization in response to stress or pharmacological stimulants after the establishment of the niche.[9,14,17-19] Recently, osteoclasts have been described as the potential regulators of HSC niche, besides their

bone-resorbing function which provides space for hematopoiesis, since they also provide signals which affect cellular and molecular components of the hematopoietic niche.[20] The association between the lack of osteoclast activity and hematopoietic defect has been studied in op/op mice and other osteopetrotic models. It was demonstrated that restoration of osteoclast function by transfer of hematopoietic stem/progenitor cells from normal mice led to rescue of bone structure, of the MSC phenotype, and of the HSC homing in the BM.[13,21-24] Mansour et al also demonstrated that osteoclasts are important for the initial niche formation and its colonization by $Lin^{neg}Sca1^{+}cKit^{+}$ (LSK) hematopoietic stem/progenitor cells (HSC/HPC) in osteopetrotic mice (oc/oc mice) through their impact on the mesenchymal compartment.[15] Osteoclasts induce formation of BM niche and its colonization by HSCs/HPCs during perinatal period by regulating the phenotype and function of MSCs and the BM vascularization. The lack of osteoclast activity in osteopetrosis results in reduced BM hematopoiesis, extramedullary hematopoiesis in the liver and spleen and progressive BM failure. The development of extramedullary hematopoiesis in osteopetrosis also suggests a strong association between HSC niche formation and functional osteoclasts. It seems that the role of osteoclasts is much more complex than just providing space for HSC niche. However, the precise role of osteoclasts remains obscure and controversial due to the use of different models and conditions.[9,15,25] For this reason, studying osteoclast biology and its impact on HSC compartment in bone marrow by using patient-derived osteopetrotic-induced pluripotent stem cells (iPSCs) have unique opportunities. Being an unlimited source of pluripotent stem cells carrying patient-specific disease-causing mutations, these patient-derived pluripotent stem cells will help to dissect disease pathogenesis and investigate new therapeutic targets through in vitro disease modeling in the laboratory, while paving the way for the development of new transplant strategies to support donor engraftment and improve outcome of transplantation in the clinic.[26] The aim of this study was to investigate alterations in mesenchymal and HSC components of the osteopetrotic BM niche using patient-derived osteopetrotic iPSCs to gain insight into abnormal hematopoiesis in osteopetrosis and stem cell dynamics/trafficking in the BM niche after HSC transplantation. To the best of our knowledge, characterization of HSC compartment of the osteopetrotic niche using human osteopetrotic iPSCs and its interaction with BM-MSCs has not been reported yet.

Materials and Methods

Generation of Induced Pluripotent Stem Cells from Peripheral Blood Mononuclear Cells

Frozen peripheral blood mononuclear cells which were isolated by density gradient separation from the peripheral blood samples of one healthy donor and 3 patients with 3 different TCIRG1 mutations were used in this study (Supplementary Table S1). Immunophenotype of isolated mononuclear cells was evaluated with flow cytometry ($CD45^{+}$ and $CD34^{neg}$, $CD36^{neg}$, $CD71^{neg}$, $CD235a^{neg}$). Erythroid progenitor cells were expanded using Erythroid Expansion Media (EEM) (StemCell Technologies), and enrichment of erythroid progenitor cells was demonstrated by flow cytometry on day 10. The data were analyzed using Beckman Coulter Navios EX Flow Cytometer (Kaluza Analysis 2.1 Software). All antibodies, cytokines, and primer sequences are shown in Supplementary Table S2.

Erythroid progenitor cells were transduced with Sendai viral vector (SeV) according to the manufacturer's instructions (CytoTune-iPS 2.0 Sendai Reprogramming Kit, Thermo Fisher Scientific, USA). Cells were fed with ReproTSR (STEMCELL Technologies) between day 5 and day 11, then maintained in TeSR-E8 (StemCell Technologies) medium starting from day 12. iPSC colonies that started to appear around day 12 after viral transduction were harvested with manual microdissection method, transferred into Matrigel-coated dishes, and were expanded with clump passaging method with EDTA.[27]

Characterization of iPSC Lines

Three iPSC lines per sample were characterized by colony morphology, immunofluorescence staining, flow cytometry and qRT-PCR. Detection of residual SeV sequences was evaluated in reprogrammed IPS cells using conventional PCR and verification of the mutations was assessed by sequencing of the genomic locus. Embryoid body formation was performed to show 3 lineage differentiation potential in vitro. Three iPSC lines were characterized for each sample.

Immunofluorescence staining was performed using PSC 4-Marker Immunocytochemistry Kit (Life Technologies). In brief, after fixation and permeabilization, iPSC colonies were first incubated with primary antibodies (OCT4, SSEA4, SOX2, and TRA1-60) for overnight, and then with conjugated secondary antibodies for 1 h at RT. Following staining with DAPI, samples were examined under fluorescence microscope (Olympus-IX73).

Immunophenotype of iPSCs was evaluated with flow cytometry (BD Accuri C6 Plus). iPSC colonies were harvested with accutase and single-cell suspensions were stained using antibodies against pluripotency markers SSEA4 and OCT4, and erythroid progenitor cell markers CD36 and CD235a.

The mRNA expression levels of the pluripotency-associated genes (Endo-OCT4, Endo-SOX2, NANOG, c-MYC, KLF-4, UTF-1, DNMT3b, TERT-1, REX-1, N-Cad) were analyzed by quantitative real-time PCR (qRT-PCR). Total RNA isolation was conducted by Promega, ReliaPrep RNA Cell Miniprep System. qPCR studies were performed using ThermoFisher Maxima SYBER Green qPCR master mix on mic qPCR cycler (Bio Molecular System, v2.6.5). Gene expression was normalized to the expressions of β-actin. The losses of Sendai virus genome (SeV genome sequence targeted) was assessed by end-point PCR using Promega GoTaq DNA polymerase. Agarose gel electrophoresis results of end-point PCR analysis were presented. Karyotype analysis was performed by G-banding to confirm the genomic stability of iPSC lines and found normal in all iPSC lines (Supplementary Fig. S4A and B).

In vitro trilineage differentiation potential of iPSC lines was evaluated with embryoid body (EB) assay. iPSC colonies were harvested using Accutase, single-cell suspensions were prepared at passage 20-24 and cells were seeded onto AggreWell800 plates (STEMCELL Technologies) in EB formation media (STEMCELL Technologies) containing 10 μM Rock inhibitor (STEMCELL Technologies). Following a 24-h suspension culture, EBs were harvested and transferred to ultra-low attachment plates in STEMdiff APEL 2 Medium (STEMCELL Technologies) and kept in culture for spontaneous differentiation. Differentiated EBs on day 7, day

14, and day 21 were characterized by IF, IHC, and RT-PCR. For immunofluorescence staining, cell aggregates were fixed for 30 min with 4% paraformaldehyde, permeabilized with 1.5% Triton X-100 for 1 h, re-fixed in 4% paraformaldehyde for 15 min, then blocked with 2% goat serum for 3 h, and incubated with primary antibodies overnight at 4 °C (α-SMA, ab7817; MAP2, ab11267; SOX17, ab192453, Abcam). Aggregates were then washed 3 times PBS and incubated with secondary antibody (Goat anti-Mouse IgG H&L (Alexa Fluor 488, abcam, ab150113). Next, aggregates were washed in PBS 3 times, stained with DAPI for 5 minutes, washed again, and imagined using confocal microscopy (CARLL ZEIS LSM 880).

For immunohistochemistry staining; cell aggregates were dehydrated through a series of graded ethanols, xylene, and paraffin before embedding into paraffin blocks. Five-micron sections, were cut and adhered to charged glass slides. Selected sections were then stained with hematoxylin and eosin. The rest of the sections were deparaffinized, rehydrated, and blocked with endogenous peroxidase, incubated with primary antibodies for one hour, then secondary antibodies for 30 minutes. After treatment with streptavidin peroxidase, and DAB, hematoxylin staining and dehydration, series of graded ethanols and xylene processes were performed, they were imagined using Olympus microscopy (Supplementary Table S1). Change in the gene expression profile of spontaneously differentiated EBs was assessed on day 7, day 14, and day 21 with RT-PCR using transcripts targeting OCT4 and α-SMA, MAP-2, and SOX17 as lineage-specific markers.

Directed Differentiation of Osteopetrotic Induced Pluripotent Stem Cells to Hematopoietic Progenitors and Osteoclasts

IPS cells at passage 20-24 were differentiated into HSCs using STEMdiff Hematopoietic Kit (STEMCELL Technologies) using a step-wise differentiation protocol which starts with induction of primitive streak/mesoderm, then hematopoietic specification and followed by hematopoietic cell maturation, myeloid cell expansion and osteoclast lineage differentiation.[28] iPSCs were passaged using EDTA clump passaging method, and 10-20 iPSC aggregates per cm^2 were plated on Matrigel coated-6-well plate in TeSR-E8 maintenance medium (STEMCELL Technologies). The cells were then incubated sequentially in STEMdiff differentiation medium containing different combinations of cytokines and hematopoietic growth factors (hVEGF, hbFGF, IL-6, IL-3, IL-11, and hSCF) for approximately 10 days. Then a fraction of the cells were harvested with acutase, and the expression of hematopoietic markers (CD43, CD34, and CD45), and also myeloid markers (CD11b, CD14, CD16, CD18, CD38, and CD115) were evaluated to show time-dependent upregulation of lineage-specific cell surface markers. Rest of the differentiated cells were used to continue myeloid-lineage differentiation and to characterize iPSC-derived hematopoietic progenitor cells (iHPCs) following the selection of $CD34^+$ cells with magnetic-activated cell sorting (Miltenyi, Cat #130-042-201), that is, colony-forming unit (CFU) assay using methocult, immunophenotyping, coculture experiments, and migration assays. The hematopoietic precursors were cultured for another 4 days to induce myeloid differentiation using StemSpan SFEM (STEMCELL Technologies)-based differentiation medium enriched with 2 mM glutamine, 4 × 10-4 M monothyioglycerol, 50 μg/mL L-ascorbic acid, 10 ng/mL hVEGF, 4 U/mL EPO, 50 ng/mL TPO, 100 ng/mL hSCF, 10 ng/mL hIL-6, 5 ng/mL hIL-11, and 40 ng/mL hIL-3 (Supplementary Table S1). Then a fraction of cells were harvested and stained with CD11b, CD14, CD16, CD18, CD34, CD38, CD43, CD45, CD115 antibodies to demonstrate the efficacy of myeloid differentiation with flow cytometry.

Hematopoietic colony-forming potential of $CD34^+$ iHPCs were assessed with semi-solid Methocult cultures (STEMCELL Technologies, MethoCult H4434 Classic). 4 × 104 cells were seeded per 35-mm culture dishes in 1.5 mL of methylcellulose, and cultured for 14 days. Colony types were determined by shape, cell size, and extent of visible erythroid content on Olympus IX73 microscope as BFU-E, CFU-G, CFU-M, CFU-GM, and CFU-GEMM. The colony counts were scored. The myeloid lineage specification and expansion of the cells were confirmed after harvesting all colonies from the dish, with lineage-specific staining with CD45, CD14, CD16, CD18, CD33, CD36, CD41 by flow cytometry.

At the final step, myeloid precursors were harvested and 1 × 105 cells/well were seeded onto Corning Osteo Assay Surface Microplate (Corning Cat#3988) in IMDM medium containing 10 ng/mL M-CSF, 10 ng/mL RANK-L, and 10% FBS. They were cultured for 21 days for induction of differentiation into functional osteoclasts. Besides immunophenotyping of the cells with monocyte-macrophage and osteoclast precursor cell markers (CD14, CD16, CD18, CD45, CD51/61), cell morphology was evaluated with scanning electron microscope (SEM FEI QUANTA 200F).

Osteoclast differentiation protocol was applied to the remaining fraction of myeloid progenitor cells. The differentiation and functionality of iPSC-derived osteoclasts was assessed by the presence of tartrate-resistant acid phosphatase activity (TRAP) activity in the multinucleated cells by immunofluorescence staining. Active functional osteoclasts were also identified by the formation of filamentous (F)-actin rings that were demonstrated by immunostaining of actin cytoskeleton with the Phalloidin conjugated to Rhodamine, and secretion of cysteine protease, cathepsin K.

Cathepsin K, NFATC1, Calcitonin R as osteoclast markers genes were analyzed with qRT-PCR at the indicated time points throughout the differentiation. The target gene normalized to the *β-actin* endogenous control, $2^{\Delta\Delta CT}$ value was calculated considering negative control, that is, healthy myeloid precursor cells.

Coculture of MSCs and iPSC-derived Hematopoietic Progenitor Cells and Migration Assay

Mesenchymal stromal cells were isolated from bone marrow samples of one healthy donor and 3 patients with 3 different TCIRG1 mutations, coculture experiments and migration assays were performed after the characterization of MSCs. The MSCs were characterized by flow cytometry (as $CD29^+$, $CD44^+$, $CD73^+$, $CD90^+$, $CD105^+$, and $CD34^{neg}$, $CD45^{neg}$). Adipogenic and osteogenic differentiation potential of hMSCs were evaluated for each established primary culture. For induction of adipocyte differentiation, cells were treated with adipogenic differentiation medium (DMEM LG (Gibco) supplemented with 10% FBS (Gibco), 1 μM dexamethasone (Sigma), 60 μM indomethacin (Sigma), 500 μM 1-methyl-3-isobutylxanthine (IBMX, Sigma), and 5 μg/mL insulin (Sigma–Aldrich) for 21 days. Then they were fixed and stained with Oil Red O stain to visualize fat droplets

within the differentiated cells. For osteoblastic differentiation, cells were treated with osteoblast induction medium (OB) containing DMEM-LG (Gibco) supplemented with 10% FBS (Gibco), 100 nM dexamethasone (Sigma), 10 mM β-glycerophosphate (Sigma), 0.2 mM ascorbic acid (Sigma) for 21 days, and Alizarin Red staining was performed to signify the osteogenic differentiation.

$CD34^+$ iPSC-derived HPCs (1 × 104 iHPCs/cm^2) enriched with magnetic-active cell sorting were cultured on a confluent layer of bone marrow-derived mesenchymal stromal cell (BM-MSCs) in CellGro SCGM supplemented with 10% FBS, 150 ng/mL FLT3-L (STEMCELL Technologies), 150 ng/mL SCF (STEMCELL Technologies), and 50 ng/mL IL-3 (STEMCELL Technologies) for 4 days. Different coculture set-ups were used to model the osteopetrotic and healthy hematopoietic niche (healthy MSC-healthy iHPCs, patient MSC-patient iHSCs, healthy MSC-patient iHPCs and patient MSC-healthy-iHPC) by using each patient' or healthy donor's own BM-MSCs and iHPCs. After 4 days, coculture plates were examined to visualize the morphology and location of iHPCs on the MSC layer by phase-contrast microscopy. Both phase-bright cells on the surface of the MSC layer and non-adherent cells were harvested and CD45 negative selection was performed by magnetic-activated cell sorting (Miltenyi) to separate MSCs from iHPCs. Flow cytometry analysis of $CD45^+$ hematopoietic cell fraction was done by using hematopoietic- and myelomonocytic-lineage-specific surface markers (CD11b, CD14, CD16, CD18, CD34, CD38, CD43, CD45, CD115) to investigate the effect of osteopetrotic MSCs on the immunophenotype and expansion of iHPCs. $CD45^{neg}$ cell fraction, that is, MSC was used to investigate the effect of osteopetrotic iHPCs on the expression of genes involved in regulation of HSCs homing and maintenance in the hematopoietic niche; Sdf-1, Jagged-1, Kit-L, Opn and other niche factors such as N-Cad, Ang-1 with qRT-PCR. Quantification of qRT-PCR signals was performed using the ($2^{-\Delta\Delta Ct}$) method,[29] which calculates relative changes in gene expression of the target gene normalized to the *β-actin* endogenous control. The values obtained were represented as the relative quantity of mRNA-level variations.

Migration assays were performed to evaluate the regulatory role of MSCs as osteoblast progenitor cells on migration and homing of iHPCs to the hematopoietic niche. A total of 1 × 106 MSCs were plated in the bottom chamber of 5-μm pore size transwells (Costar) with MEM-α medium containing 10% FBS and incubated at 37 °C and 5% CO_2. After 24 h, MSCs were labeled with CellTracker Green CMFDA (ThermoFisher), and $CD34^+$ iHPCs labeled with CellTracker Orange CMTMR (ThermoFisher) were plated in transwell inserts. After 4h of incubation at 37 °C and 5% CO_2, remaining cells at the transwell inserts were removed and cells migrated to the bottom chambers were visualized and quantified by Olympus IX73 fluorescence microscope.

Statistical Analysis

Arbitrary gene expression levels were achieved by normalizing the gene of interest to the geometrical mean expressions of reference genes as described previously.[26,30] The arbitrary gene expression was further normalized to the mean expression of control samples to achieve fold change values. The results of different parameters were presented as mean + SEM. The comparisons between the groups were done by using unpaired or paired 2-tailed *t* test. Friedman multiple comparisons test, and one sample Wilcoxon test were used for time-course experiments. Kruskal-Wallis multiple comparisons test was applied to independent multiple groups comparisons. Analysis of variance was conducted on the replicate values of experiment groups. *P* values <0.05 were accepted as statistically significant. The data were analyzed using GraphPad Prism 8.01.

Results

Generation of Induced Pluripotent Stem Cells from Peripheral Blood Erythroid Progenitors of Osteopetrotic Patients

Peripheral blood mononuclear cells (PBMCs) obtained from 3 patients with 3 different mutations of TCIRG1 gene and one healthy donor were enriched for erythroid progenitor cells before reprogramming with CytoTune Sendai reprogramming kit. Enrichment efficiency of erythroid progenitors derived from the patients' samples was confirmed by flow cytometry [CD36 (95.9% ± 1.6), CD71 (98.5% ± 0.15), and CD235a (72.4% ± 8.78) (Supplementary Fig. S1A, B)]. The first osteopetrotic iPSC colonies were observed at around days 12-15 after transduction. Eight to 10 iPSC colonies from each iPSC line established were picked manually and expanded in culture for detailed analyses (Supplementary Fig. S1C).

All iPSC lines derived from the osteopetrosis patients and the healthy donor expressed pluripotency markers (SSEA4, OCT3/4, TRA1-60, SOX2) as assessed by immunofluorescence staining (Supplementary Fig. 1A), and flow cytometry (SSEA4, OCT3/4). More than 90% of iPSCs were positive for OCT4 (patients 95.2% ± 1.57; healthy 92.6% ± 3.55), and SSEA4 (patients 99.07% ± 1.73; healthy 98.86% ± 0.57), while they were either negative or weak positive for CD36 (patients 4.1% ± 1.73; healthy 3.06% ±1.13) and for CD235a (patients 1.71% ± 0.57; healthy 1.33% ± 0.55) (Supplementary Fig. 1B). The pluripotency-associated gene expression profiles were evaluated with a panel of 10 different target genes including OCT4, SOX2, c-MYC, KLF4, N-Cad, REX1, TERT1, UTF1, DNMT1, NANOG (Supplementary Fig. S2A). Post-reprogramming mutation verification analysis was also performed and showed that disease-related mutations were retained in all iPSC lines (Supplementary Fig. 1C).

Trilineage differentiation potential of generated iPSC lines were evaluated with embryoid body (EB) formation and ability of iPSC-derived EBs to give rise to early progenitors belonging to each of 3 germ layers. Spontaneously differentiated EBs were stained triple-positive with lineage-specific MAP2 (ectoderm, neural lineage marker), α-SMA (mesoderm, mesenchymal stromal cell marker), SOX17 (endoderm, fetal hematopoetic stem cell marker) on day 21 by immunofluorescence staining (Fig. 1D) Lineage-specific gene expression profiles were shown in Supplementary Fig. S2B-D.

Hematopoietic Differentiation Potential of Osteopetrotic iPSCs Shifted Toward Monocyte-Macrophage Lineage

Osteopetrotic iPSCs were differentiated into hematopoietic progenitor cells (HPC) using a step-wise protocol. Hematopoietic cell clusters appeared starting from day 3 of culture and progressively increased in number and size up to day 10 finally giving radial-sac like structures (Fig. 2A). Majority of the multipotent hematopoietic progenitors (>85%) co-expressed CD34 and CD45, and myelomonocytic markers albeit at low levels [$CD34^+CD45^+$ (healthy 93.6%; patients 90.3% ±

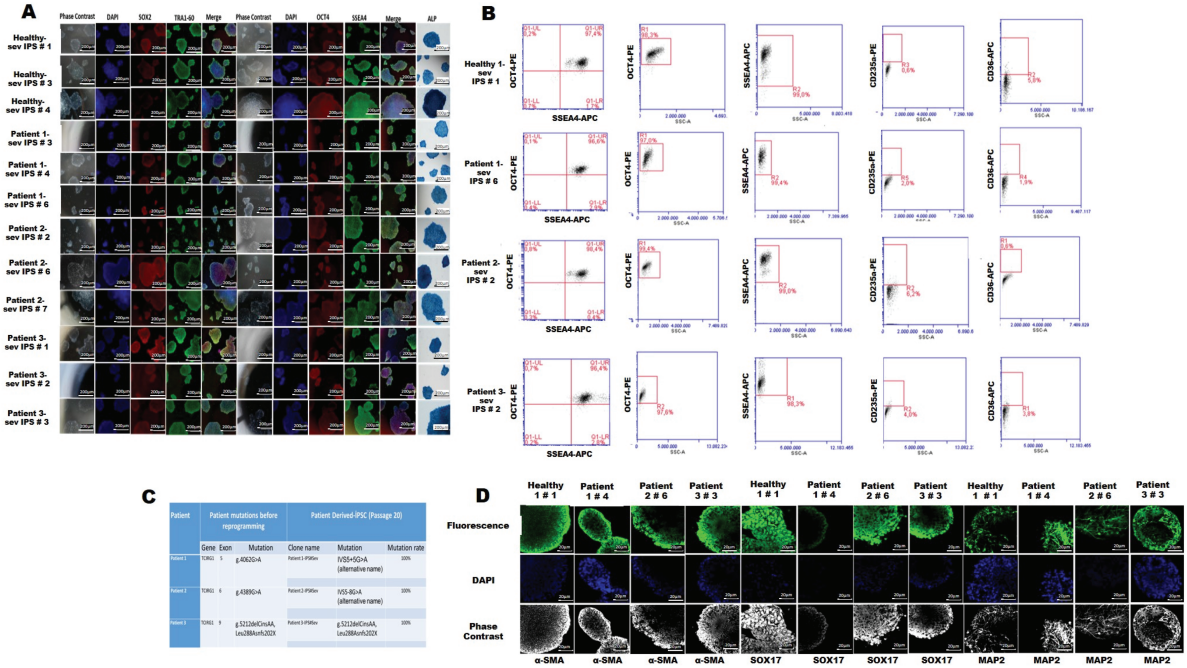

Figure 1. Characterization of established iPSC lines derived from patient and healthy control peripheral blood erythroid precursors. (A) Immunofluorescence and ALP staining of 3 different clones of each of the selected iPSCs lines. (B) Flow cytometry analysis with pluripotency markers; OCT4, SSEA4, and erythroid progenitor cell surface markers, CD36 and CD235a after reprogramming. (C) Verification of persistence of 3 different TCIRG1 mutations in osteopetrotic iPSCs. (D) Immunostaining of spontaneously differentiated iPSCs-derived embryonic bodies with lineage-specific markers; MAP2 (ectoderm), α-SMA (mesoderm), SOX17 (endoderm).

2.05), CD11b (healthy 29.4%; patients 44.06% ± 5.7), CD14 (healthy 26%; patients 22.16% ± 3.7), CD16 (healthy 14%; patients 9.9% ± 1.7), CD18 (healthy 14.9%; patients 16.6% ± 1.9), CD38 (healthy 44%; patients 50.8% ± 2.6), CD43 (healthy 90.8%; patients 92.9% ± 6.2) (Fig. 2B) Both healthy- and osteopetrotic-iHPCs (purity ≥94% after $CD34^+$ selection) formed granulocyte/macrophage (CFU-M, CFU-G, and CFU-GM), and rare mixed (CFU-GEMM) colonies (Fig. 2C). BFU-E colonies were formed only by healthy-iHSCs whereas osteopetrotic-iHPCs showed a 3-fold increase in macrophage colony-forming ability (CFU-M). Flow cytometry analysis of hematopoietic colonies revealed a distinct hematopoietic differentiation potential of osteopetrotic iHPCs shifting toward monocyte-macrophage lineage [CD14 (healthy 32.6%; patient 50.9 ± 3.5%), CD16 (healthy 20.6%; patient 36.7 ± 5.9%), CD18 (healthy 7.8%; patient 35.03 ± 3.6%), CD33 (healthy 81.9%; patient 84.2 ± 7.4%), CD36 (healthy 81%; patient 69.13 ± 3.9%), CD41 (healthy 7.9%; patient 23.03 ± 5.1%) (Fig. 2D). Multipotent hematopoietic progenitors were further differentiated into myeloid precursors by culturing with erythropoietin and thrombopoietin containing differentiation medium for another 4 days (Fig. 2F). Myeloid-enriched progenitor cells ($CD34^+CD43^+CD45^+$) was declined from 90.1 ± 5.1% to 52.6 ± 8.9% following differentiation and expansion and those of expressing monocyte-macrophage lineage-specific markers were increased more significantly by day 14 [(CD11b from 44 ± 3.3% to 60.4 ± 4.5%), CD14 (from 22.2 ± 3.7% to 52.9 ± 0.4%), CD16 (from 9.9 ± 1% to 55.9 ± 1.7%), CD18 (from 16.6 ± 2% to 46.8 ± 4.2%)} (Fig. 2E) for patient iHPCs ($P < .05$). Also, monocyte-macrophage lineage-specific markers expression of patient iHPCs-derived myeloid cells were significant higher comparing to healthy myeloid cells [CD11b (healthy 42.9; patient 60.4 ± 4.5), CD14 (healthy 38.2; patient 52.9 ± 0.4), CD16 (healthy 27.2; patient 55.9 ± 1), CD18 (healthy 25.2; patient 46.8 ± 4.2), $P < .05$].

Osteopetrotic iPSC-derived Myelomonocytic Precursors Generate Dysfunctional Osteoclasts

We next investigated whether myelomonocytic precursors derived from osteopetrotic iPSCs had the potential to differentiate further into mature osteoclasts. iPSC-derived myelomonocytic precursors were seeded onto multiple-well plates coated with a synthetic inorganic bone mimetic and cultured in the presence of M-CSF and RANKL, which are essential cytokines for osteoclasts differentiation and survival. Change in cell morphology and size was observed throughout the culture and multinucleated cells were formed at the end of the differentiation period (Fig. 3A). Osteopetrotic-iPSC-derived multinucleated osteoclasts were phenotypically similar to healthy osteoclasts and demonstrated similar expressions of CD14 (healthy 98.3%, patient 99.1 ± 0.3%), CD16 (healthy 98.2%, patient 88.3 ± 3.7%), CD18 (healthy 96.6%; patient 99.5 ± 0.5%), CD51/61 (healthy 100%; patient 78.8 ± 7.6%), which are specific surface markers for osteoclast precursors (Fig. 3B). The identity and functionality of differentiated osteoclasts were confirmed by the presence of TRAP activity and secretion of a cysteine protease Cathepsin K, enzymes highly expressed in mature osteoclasts. We further examined the formation of F-actin rings which are specific cytoskeletal structures of resorbing active osteoclasts (Fig. 3C). TRAP-positive osteopetrotic-osteoclasts had weak actin ring formation and decreased Cathepsin K secretion compared with healthy osteoclasts. The electron microscope images indicated a difference between the podosome sizes of osteopetrotic and healthy multinucleated osteoclasts (Fig. 3C). There was a significant reduction in the expression

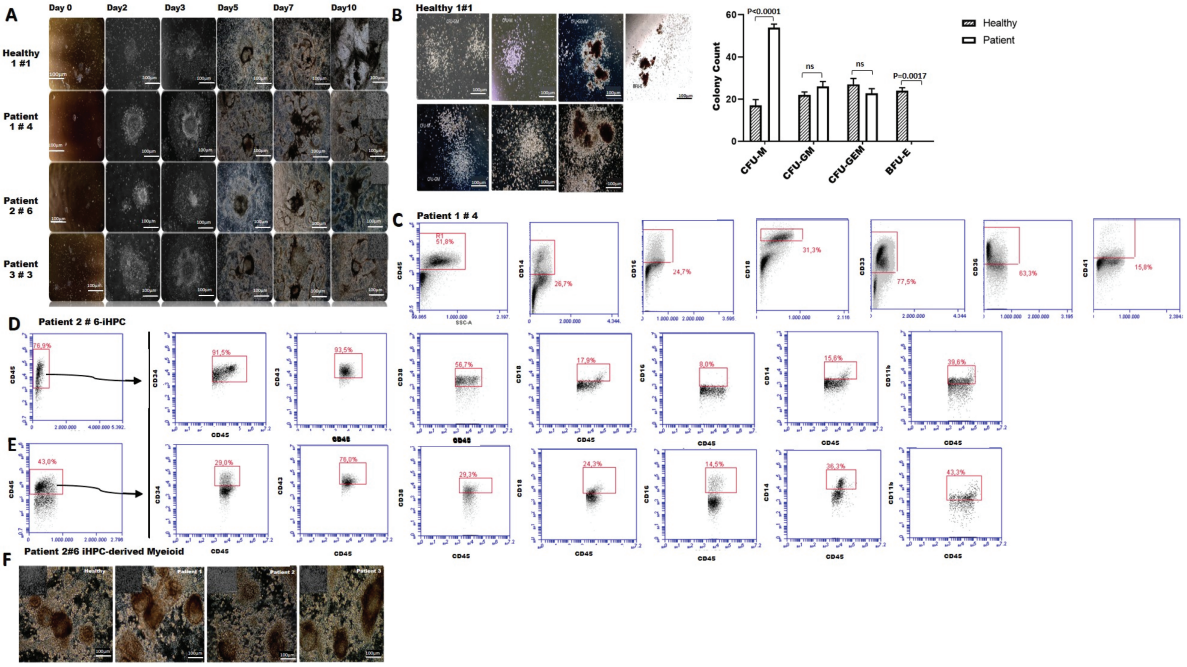

Figure 2. Assessment of hematopoietic differentiation potential of iPSC lines. (A) Differentiated blood-forming hematopoietic progenitor cells colonies with the formation of radial sac-like structures. (B) Confirmation of the clonogenic potential of iHSCs by CFU assay; healthy iPSCs-derived hematopoietic colonies (upper row), patient iPSCs-derived hematopoietic colonies (lower row). (C) Confirmation of hematopoietic lineage commitment of cells forming colonies by flow cytometry after methocult assay. (D) Flow cytometry analyses of osteopetrotic iPSCs that are differentiated to hematopoietic progenitor cells as indicated by an increase in $CD34^+CD45^+$ cell fraction by day 10 following hematopoietic induction coupled with low expression of myelomonocytic markers (CD14, CD16, CD18, 11b, CD38, and CD43). (E) Flow cytometry analysis shows a distinct pattern of differentiation in osteopetrotic iHSCs toward monocyte-macrophage lineage at day 14. (F) Morphological evaluation of hematopoietic progenitors differentiated toward myeloid lineage.

levels of osteoclast-specific genes; Cathepsin-K, Calcitonin-R, and NFATC1 in osteopetrotic osteoclasts as compared with healthy osteoclasts (Fig. 3D). Overall, osteopetrotic osteoclasts which are phenotypically identical to healthy osteoclasts were found functionally defective.

Impaired Differentiation Potential, Homing and Retention of Osteopetrotic HPCs Recover After Coculture with Healthy MSCs

Mesenchymal stromal cells are critical components of the hematopoietic niche and remain in close contact with cells of hematopoietic origin including osteoclasts. They play important role in hematopoiesis by regulating maintenance, proliferation, differentiation of hematopoietic stem/progenitor cells through the secretion of soluble factors and cell-cell contact.[31,32] They are the progenitors of bone-forming osteoblasts which are required for hematopoietic niche formation. Osteoclasts regulate the phenotype and function of MSCs and induce their osteoblastic commitment.[15] Thus, alterations in the HPC compartment in the bone marrow of osteopetrosis patients could be related to modifications in MSCs. To test this hypothesis, we established a coculture system with iHPCs and bone marrow-MSCs of osteopetrosis patients to model these niche compartments in vitro. First, bone marrow-MSCs were characterized by morphology, immunophenotyping and assessment of their differentiation potency. All MSCs lines expressed specific surface markers of mesenchymal stromal cells and they were negative for hematopoietic markers (Supplementary Fig. S3B). However, diminished osteogenic differentiation potential was detected by histochemical staining in osteopetrotic BM-MSCs (Supplementary Fig. S3A). When immunophenotypes of CD34-enriched healthy iHPC cocultured with healthy MSCs (as in healthy niche) and osteopetrotic iHPCs cocultured with osteopetrotic MSCs (as in osteopetrotic niche) were compared, we found a significant difference among the expressions of myelomonocytic progenitor and differentiation markers, confirming the a distinct differentiation potential of osteopetrotic iHPCs shifting toward monocyte-macrophage lineage [$CD34^+CD43^+CD45^+$ (healthy 27.8%; patient 52.1 ± 15.4%), CD11b (healthy 35.6%; patient 66.8 ± 9.2%), CD14 (healthy 19.7%; patient 64.8 ± 9.3%), CD16 (healthy 8.1%; patient 23.6 ± 5.45%), CD18 (healthy 33.5%; patient 81.1 ± 8.8%), $P < .05$] (Fig. 4A). Next, we performed coculture experiments with iHPCs and MSCs to address the alterations in osteopetrotic iHPCs. We observed an increase in the proportion of $CD34^+$ and $CD38^+$ hematopoietic progenitor cells in osteopetrotic iHPCs cocultured with healthy MSCs ($CD34^+$ cells; 37.8% ± 9.9 vs. 52.4% ±12.15, $P > .05$, $CD38^+$ cells; 35.8% ± 5.2, vs. 62.9% ± 1.6, $P < .05$). The frequency of $CD14^+$ (64.8% ± 9.3 vs. 29.03% ± 5.05, $P < 0.0001$) and $CD18^+$ (81.1% ± 8.8 vs. 63.3% ± 12.4, $P > 0.05$) myeloid progenitors was lower. On the other hand, healthy iHPCs cocultured with osteopetrotic MSCs showed a shifted differentiation toward monocyte-macrophage lineage compared with their phenotype after coculture with healthy MSCs ($CD34^+CD43^+CD45^+$, 42.7% ± 2.3 vs. 27.8% ± 3.1; $CD14^+$, 37.3% ± 2.7 vs. 19.7% ± 2.9; CD18+, 46.4% ± 3.4 vs. 33.5% ± 3.2, $P < 0.05$). Altogether these data demonstrate that there is an alteration in the hematopoietic differentiation potential of osteopetrotic HPCs.

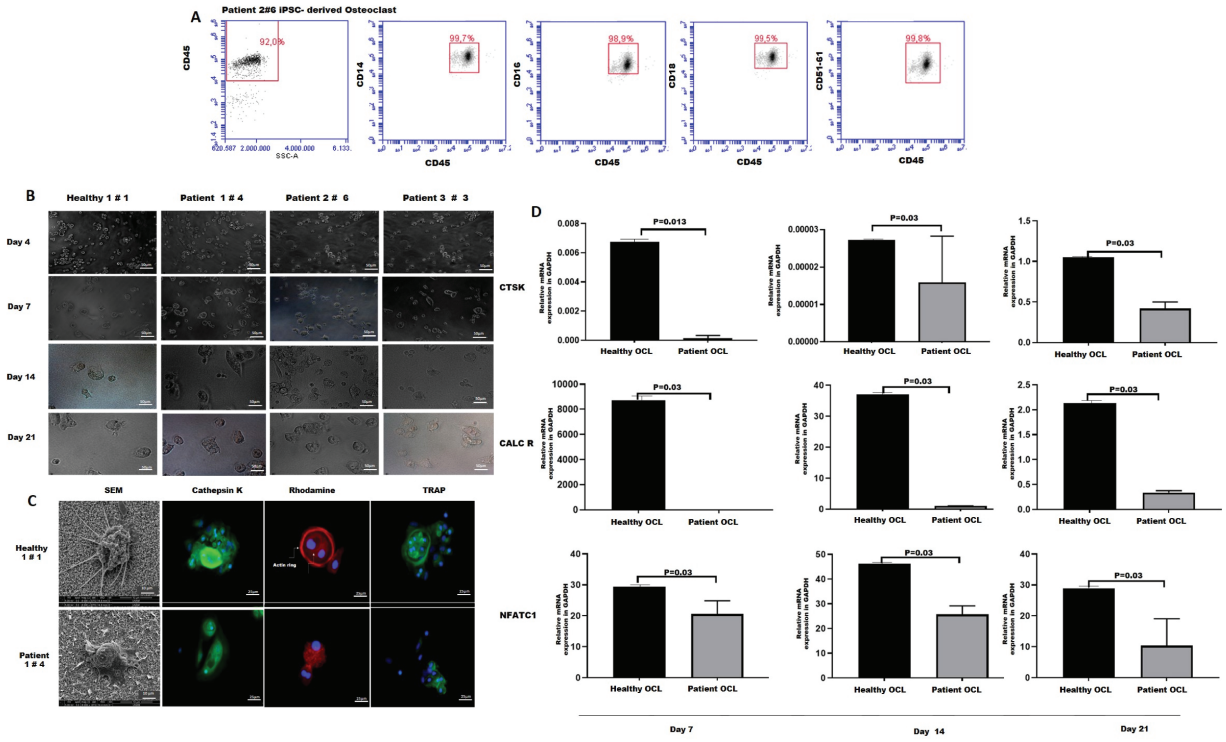

Figure 3. Differentiation of osteoclasts from iPSC-derived myelomonocytic precursors. (A) Phenotyping of osteoclasts derived from iPSCs indicates an increase in osteoclast progenitor cell markers (CD14, CD16, CD18, CD45, CD51/6). (B) Representative images demonstrating the changes in cell morphology throughout the differentiation process (50 μm magnification). (C) Scanning electron microscope imaging of iPSCs-derived-osteoclasts (10 μm magnification), and immunofluorescence staining (Cathepsin K, Rhodamine, TRAP) showing the functionality of osteoclasts (25 μm magnification) (left hand panel-healthy, right hand panel-patient). (D) qRT-PCR analysis for expression of osteoclast-specific CTSK, CALCR, and NFATC1 genes. Bar graphs indicates mean ± SD of duplicates from 3 patients. Differences at different time points were evaluated with Wilcoxon test.

This alteration could be a rescue mechanism for defective osteoclast function in osteopetrosis. The restoration of the skewed phenotype of osteopetrotic iHPCs after co-culturing with healthy MSCs supports the impairment in osteopetrotic MSCs.[1,13,33]

To gain more insight into the regulatory role of MSCs in HSC niche, we analyzed the expression of genes controlling HSC homing, survival, quiescence and adhesion such as Ang-1, Kit ligand (Kit-L), Sdf-1, Jag-1, Opn, and N-Cad in osteopetrotic MSCs after coculture with osteopetrotic iHPCs. Osteopetrotic MSCs showed lower expression of Ang-1, Jag-1, Sdf-1, Opn, and higher expression of N-Cad when cocultured with osteopetrotic iHPCs in comparison with the healthy MSCs cocultured with healthy iHPCs. Interestingly, the expression of Jag-1, Kit-L, and Opn was significantly increased and N-Cad decreased after coculture with healthy iHPCs (Fig. 4B). These results suggest an alterations in MSCs function in supporting HSCs.

Finally, we performed in vitro migration assay to investigate the ability of osteopetrotic MSCs to attract HSCs. A dramatic reduction in attraction ability of osteopetrotic MSCs was observed for both osteopetrotic and healthy iHPCs compared with healthy MSCs. Contrarily, the migratory potential of osteopetrotic- iHPCs was significantly recovered after coculture with healthy MSCs. (Fig. 4C, D). Accordingly, these results confirm that MSC compartment was altered in osteopetrosis and this alteration results in defective homing of hematopoietic progenitors and decrease in the size of HSC pool.

Discussion

Osteoclast dysfunction and defective bone resorption in MIOP lead to skeletal, neurological and hematological abnormalities often necessitating HSCT.[1,34] The hematological defects have been attributed to the decrease in bone marrow space. However, recent reports suggest a regulatory role for osteoclasts in the HSC niche providing signals which affect cellular and molecular components of the hematopoietic niche.[13,15]

The present study was performed to investigate the hematopoietic niche and HSC interactions in patients with MIOP to delineate the contribution of niche dysfunction to osteoclastogenesis, occurrence of hematological abnormalities, and engraftment failure after HSC transplantation. Cocultures were performed with MSCs, the essential components of the BM stroma, and the HPCs of patients and healthy control cells. Previous studies have demonstrated that, in HSCT, in spite of achievement of full donor hematopoietic chimerism, the BM-MSCs remain of host type.[35] Therefore, we hypothesized that MSC dysfunction in the osteopetrotic niche may impair engraftment of healthy donor cells, thus contribute to engraftment defects after transplantation.

In HSCT, following infusion of the stem cell product, donor HSC/HPCs home to the hematopoietic niche in the marrow and through adhesive interactions with the cells and the extracellular matrix, reside in the BM niches to provide lifelong hematopoiesis of donor type. Homing and retention are mediated through receptor-ligand interactions between cells,

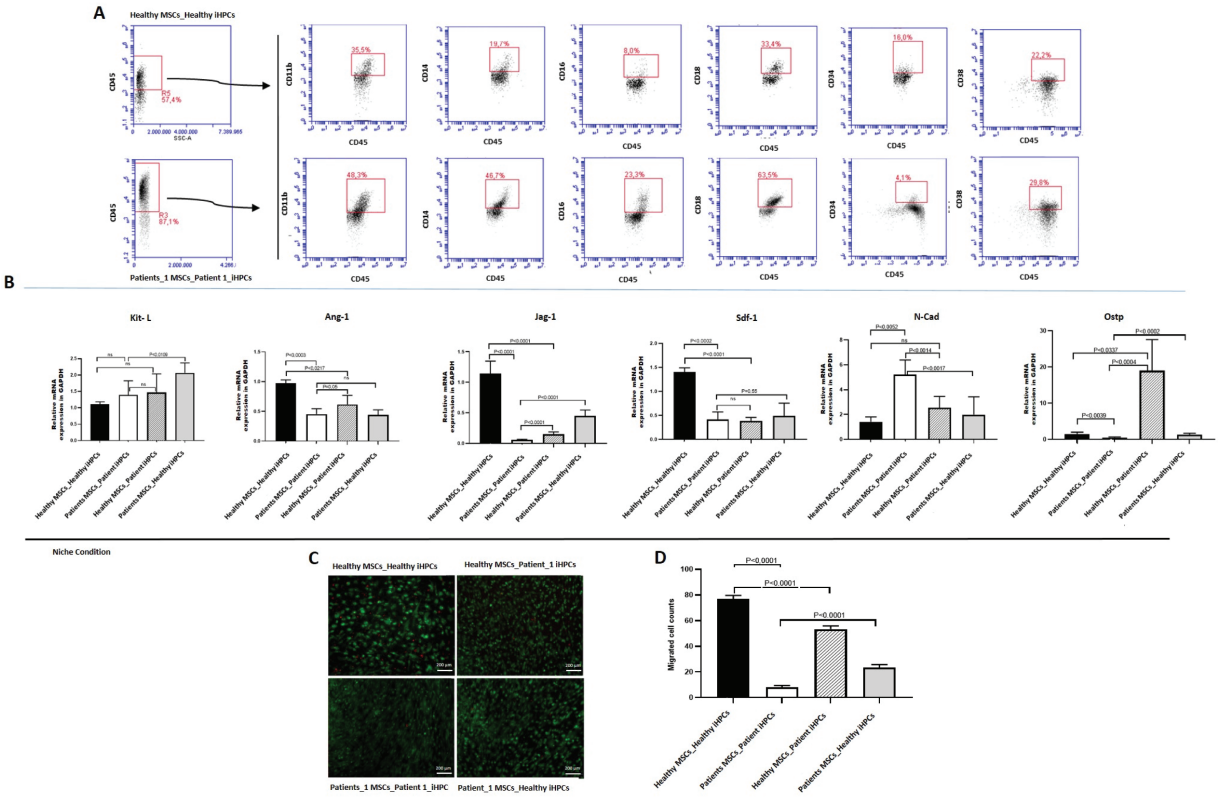

Figure 4. Coculture of BM-MSCs and iHPCs; evaluation of immunophenotype, migration potential of iHSCs and gene expression profile of BM-MSCs. (A) Representative figure shows alteration of hematopoietic and myeloid-lineage-specific surface markers after coculture (upper row: healthy iHPCs cocultured with healthy MSCs, lower row: patient iHPCs cocultured with patient MSCs) (Patient 1#4 iPSC-derived HPC, unpaired 2-tailed T test). (B) Evaluation of the expression of genes involved in the regulation of hematopoietic stem/progenitor cells in the hematopoietic niche; Sdf-1, Jagged-1, N-Cad, Ang-1, Kit-L, Opn in osteopetrotic MSCs after coculture with qRT-PCR. (Bar graphs indicates mean ± SD of duplicates from 3 patients). (C) Osteopetrotic iHPCs demonstrated a diminished migratory ability which was recovered after coculture with healthy MSCs. (D) Bar graph shows the mean number of migrated HPCs (mean ± SD of 2 replicates for 3 patients and one healthy control. Unpaired 2-tailed *t* test was used for comparison).

the extracellular matrix and through chemokine, cytokine, growth factor, adhesion molecule interactions.[36,37] MSCs, being the precursors of osteoblasts, adipocytes and due to their secretory functions play active roles in homing, retention, migration, differentiation and mobilization of HSCs.[31,32] Therefore, in the present study MSCs were used in coculture experiments to represent niche stromal cells.

Osteoclasts are derived from the hematopoietic lineage. In the BM, osteoclasts are in close interaction with MSCs and osteoblasts, both of which are important in their differentiation from monocyte-macrophage precursor and function.[16,38] In this study, we reprogrammed peripheral blood mononuclear cells of osteopetrosis patients carrying different mutations in TCIRG1 gene and successfully generated osteoclasts from patient-derived iPSCs. They were phenotypically identical to healthy osteoclasts but have defective maturation as expected since TCIRG1 mutation affects osteoclast function due to impaired ruffled border formation.[2,39] NFATc1 is a master transcription regulator which is responsible from terminal osteoclast differentiation. It promotes osteoclast-specific gene expressions which are required for differentiation and bone resorption, such as Calcitonin receptor, Cathepsin K and TRAP.[40,41] We observed thinner actin ring formation, weak TRAP activity and decreased Cathepsin K secretion correlated with decreased NFATC1 expression in osteopetrotic-osteoclasts comparing with healthy osteoclasts. This data indicate that osteoclasts from patients with TCIRG1 mutation could not differentiate into actively resorbing mature osteoclasts.[41] Interestingly, when patient-derived iPSCs were differentiated into hematopoietic progenitor cells, they showed an increase in macrophage colony-forming ability (CFU-M) compared with healthy iHPCs. Further differentiation of osteopetrotic iHPCs into myeloid progenitors gave rise to more monocyte-macrophage progenitors, revealing a distinct hematopoietic differentiation potential of osteopetrotic iPSCs which leads to enrichment of monocyte-macrophage progenitors. Augmented intra- and extramedullary myelopoiesis together with an increase in osteoclastogenesis was reported in oc/oc mice.[42]The upregulation of the myelomonocytic differentiation of osteopetrotic iHPCs may present a compensatory mechanism for the lack of bone-resorbing active osteoclasts. Since hematopoiesis is regulated by bone marrow niche and stress conditions such as irradiation, infections or drugs which change heterogeneity of hematopoietic stem/progenitor cells and hematopoietic hierarchy, skewed differentiation potential of osteopetrotic iHPCs probably develops as a response to perturbation in the balance between bone-resorbing and bone-forming cells in osteopetrosis.[43,44] Also, in vitro monocyte-macrophage lineage enrichment of osteopetrotic iHPCs even in the absence of MSCs may suggest intrinsic contribution of osteopetrotic hematopoietic progenitors.

In our study, osteopetrotic MSCs expressed Ang-1, Sdf-1, Jag-1, Opn, the genes associated with HSC homing and

maintenance in bone marrow at low levels.[45-49] Furthermore, their ability to attract HPCs was dramatically impaired. The decreased expression of main regulators of HSC proliferation, quiescence, and homing in osteopetrotic MSCs as well as their impaired attraction ability over HPCs are most likely the mechanisms behind defective HSC homing, and loss of hematopoietic progenitors in bone marrow of osteopetrosis patients. Interestingly, N-cadherin expressed in bone marrow stromal progenitors that are needed for reservation of HSCs in niche, especially under stress, was found overexpressed in osteopetrotic MSCs. This could be a stress response to impaired hematopoiesis in osteopetrosis to support HSC maintenance in bone marrow niche,[50] although N-cadherin does not play an essential functional role in HSCs.[51] In addition, the expression of Jag-1, Kit-L, and Opn in osteopetrotic MSCs was significantly increased and N-Cad decreased upon coculture with healthy iHPCs. These results suggest a functional impairment in MSCs regarding their role in HSC homing and maintenance and confirm their role in defective hematopoietic niche formation in osteopetrosis through their interaction with dysfunctional osteoclasts. The restoration of function of osteopetrotic MSCs and altered phenotype of osteopetrotic hematopoietic progenitors after coculture with their healthy counterparts point out that osteoclasts play a key role in all these modifications. This data may be a proof of concept for clinical studies which evaluate the feasibility/safety of MSC co-transplantation in osteopetrosis patients undergoing allogeneic HSC transplantation to facilitate engraftment through their support on the recovery of abnormal bone marrow niche and HSC homing.

Considering the need for newer strategies to improve engraftment status in MIOP, we previously performed a clinical study in which co-infusion of MSCs with HSCT in 12 children led to improvement in engraftment and survival, when compared with historical controls.[6] This observation is in accordance with the results of our present study demonstrating correction of hematopoietic defects upon culturing with healthy MSCs and suggests the presence of MSC dysregulation in patients with MIOP. In addition to the MSC alterations affecting HSC homing, adhesion, retention and differentiation, we also found reduced osteogenic potential of MSCs of MIOP patients. This data seems to be contradicting the results of the previous study from our group which demonstrated lack of adipocytic differentiation in BM-MSCs of 5 out of 6 patients with osteopetrosis, suggested to be resulting from the mechanical stress in the compact BM microenvironment in MIOP.[11] On the other hand, the MSC differentiation experiments in the current study revealed diminished osteogenic differentiation by histochemical staining, in our 3 patients cohort. The number of patients is very small to make definitive comments; however, the different results can be attributed to the impact of different osteopetrosis mutations, disease phenotype, age of patient, characteristics of the BM microenvironment at the time of BM aspiration, and heterogeneity of ex vivo expanded BM-MSCs. Considering the extremely rare occurrence of MIOP and the difficulty in obtaining BM samples due to the sclerotic bone properties, investigations on human BM samples is challenging, and this could be is a potential limitation of our study. However, the findings in the present study demonstrating correction of myeloid phenotype and migratory potential of HPCs, together with the presence of a variety of MSC differentiation defects highly suggest the presence of a dysregulated BM niche in MIOP patients pointing out a favorable role for MSC co-infusion in HSCT practice.

Conclusion

Our results establish the existence of significant alterations in both MSC and HPC compartments of hematopoietic niche in osteopetrosis patients. Restoration of osteopetrotic MSCs function and altered phenotype of osteopetrotic hematopoietic progenitors upon coculture with their healthy counterparts point out the regulatory role of osteoclasts in hematopoietic niche. Modeling of osteoclastogenesis and hematopoietic niche compartments with patient-derived iPSCs improve our knowledge about abnormal hematopoiesis in osteopetrosis and provide a research platform to investigate new therapeutic targets while paving the way for the development of new transplant strategies in clinic.

Acknowledgments

We are thankful to Jean J. Kim, PhD (Director) for providing expertise and Human Stem Cell Core of Baylor College of Medicine for continuous technical support. We also thank Dr Aytekin Akyol for his assistance with H&E and immunohistochemical stainings.

Funding

This study is supported by The Scientific and Technological Research Council of Turkey (TUBITAK), 1003-Primary Subjects R&D Funding Program, Project No:213S181, and 1001-The Scientific and Technological Research Projects Funding Program, Project No: 117S145.

Conflict of Interest

The authors declare no potential conflict of interests.

Author Contributions

F.V.O., D.U.C. conceived the project. They contributed equally as co-corresponding authors. F.V.O. and I.C.Z. designed, and performed the experiments and analyzed the data. B.A., C.O. performed the experiments. F.V.O. and D.U.C. designed the patient sample collection and collected the patient samples. All authors approved the final draft and made modifications to the text.

Data Availability

All data are available through the corresponding author upon request.

Ethics Approval and Consent to Participate

Written informed consent for the collection, storage and use of cells for research purposes were obtained and the study is approved by the Institutional Review Board of Hacettepe University (Study approval number: GO 16/562-08).

Supplementary Material

Supplementary material is available at *Stem Cells Translational Medicine* online.

References

1. Sobacchi C, Schulz A, Coxon FP, et al. Osteopetrosis: genetics, treatment and new insights into osteoclast function. *Nat Rev Endocrinol*. 2013;9(9):522-536.
2. Frattini A, Orchard PJ, Sobacchi C, et al. Defects in TCIRG1 subunit of the vacuolar proton pump are responsible for a subset of human autosomal recessive osteopetrosis. *Nat Genet*. 2000;25(3):343-346.
3. Palagano E, Menale C, Sobacchi C, et al. Genetics of osteopetrosis. *Curr Osteoporos Rep*. 2018;16(1):13-25.
4. Zirngibl RA, Wang A, Yao Y, et al. Novel c. G630A TCIRG1 mutation causes aberrant splicing resulting in an unusually mild form of autosomal recessive osteopetrosis. *J Cell Biochem*. 2019;120(10):17180-17193.
5. Orchard PJ, Fasth AL, Le Rademacher J, et al. Hematopoietic stem cell transplantation for infantile osteopetrosis *Blood* 2015;126(2):270-276.
6. Tavil B, Karasu G, Kuskonmaz B et al. *Mesenchymal stem cell therapy in malign infantile osteopetrosis: Hacettepe experience from Turkey*. 2015.
7. Del Fattore A, Capannolo M, Rucci N. Bone and bone marrow: the same organ *Arch Biochem Biophys*. 2010;503(1):28-34.
8. Teti A. Osteoclasts and hematopoiesis. *Bonekey Reports*. 2012;1:46.
9. Lymperi S, Ersek A, Ferraro F, et al. Inhibition of osteoclast function reduces hematopoietic stem cell numbers in vivo. *Blood*. 2011;117(5):1540-1549.
10. Mansour A, Abou-Ezzi G, Sitnicka E, et al. Osteoclasts promote the formation of hematopoietic stem cell niches in the bone marrow. *J Exp Med*. 2012;209(3):537-549.
11. Uckan D, Kilic E, Sharafi P, et al. Adipocyte differentiation defect in mesenchymal stromal cells of patients with malignant infantile osteopetrosis. *Cytotherapy*. 2009;11(4):392-402.
12. Alkhayal Z, Shinwari Z, Gaafar A, et al. Proteomic profiling of the first human dental pulp mesenchymal stem/stromal cells from carbonic anhydrase II deficiency osteopetrosis patients. *Int J Mol Sci*. 2021;22(1):380.
13. Blin-Wakkach C, Rouleau M, Wakkach A. Roles of osteoclasts in the control of medullary hematopoietic niches. *Arch Biochem Biophys*. 2014;561:29-37.
14. Winkler IG, Sims NA, Pettit AR, et al. Bone marrow macrophages maintain hematopoietic stem cell (HSC) niches and their depletion mobilizes HSCs. *Blood*. 2010;116(23):4815-4828.
15. Mansour A, Abou-Ezzi G, Sitnicka E, et al. Osteoclasts promote the formation of hematopoietic stem cell niches in the bone marrow. *J Exp Med*. 2012;209(3):537-549.
16. Jacome-Galarza CE, Percin GI, Muller JT, et al. Developmental origin, functional maintenance and genetic rescue of osteoclasts. *Nature*. 2019;568(7753):541-545.
17. Adams GB, Chabner KT, Alley IR, et al. Stem cell engraftment at the endosteal niche is specified by the calcium-sensing receptor. *Nature*. 2006;439(7076):599-603.
18. Kollet O, Dar A, Shivtiel S, et al. Osteoclasts degrade endosteal components and promote mobilization of hematopoietic progenitor cells. *Nat Med*. 2006;12(6):657-664.
19. Peled A, Petit I, Kollet O, et al. Dependence of human stem cell engraftment and repopulation of NOD/SCID mice on CXCR4. *Science*. 1999;283(5403):845-848.
20. Kollet O, Dar A, Lapidot T. The multiple roles of osteoclasts in host defense: bone remodeling and hematopoietic stem cell mobilization. *Annu Rev Immunol*. 2007;25:51-69.
21. Nilsson SK, Johnston HM, Whitty GA, et al. Osteopontin, a key component of the hematopoietic stem cell niche and regulator of primitive hematopoietic progenitor cells. *Blood*. 2005;106(4):1232-1239.
22. Nakamichi Y, Mizoguchi T, Arai A, et al. Spleen serves as a reservoir of osteoclast precursors through vitamin D-induced IL-34 expression in osteopetrotic op/op mice. *Proc Natl Acad Sci USA*. 2012;109(25):10006-10011.
23. Frattini A, Blair HC, Sacco MG, et al. Rescue of ATPa3-deficient murine malignant osteopetrosis by hematopoietic stem cell transplantation in utero. *Proc Natl Acad Sci USA*. 2005;102(41):14629-14634.
24. Cackowski FC, Anderson JL, Patrene KD, et al. Osteoclasts are important for bone angiogenesis. *Blood*. 2010;115(1):140-149.
25. Mansour A, Wakkach A, Blin-Wakkach C. Role of osteoclasts in the hematopoietic stem cell niche formation. *Cell Cycle*. 2012;11(11):2045-2046.
26. Okur FV, Cevher I, Özdemir C, et al. Osteopetrotic induced pluripotent stem cells derived from patients with different disease-associated mutations by non-integrating reprogramming methods. *Stem Cell Res Ther*. 2019;10(1):1-10.
27. Hartung O, Huo H, Daley GQ, et al. Clump passaging and expansion of human embryonic and induced pluripotent stem cells on mouse embryonic fibroblast feeder cells. *Curr Protoc Stem Cell Biol*. 2010;14(1):1C.10.11-11C.10.15.
28. Grigoriadis AE, Kennedy M, Bozec A, et al. Directed differentiation of hematopoietic precursors and functional osteoclasts from human ES and iPS cells. *Blood*. 2010;115(14):2769-2776.
29. Livak KJ, Schmittgen TD. Analysis of relative gene expression data using real-time quantitative PCR and the 2−ΔΔCT method. *Methods*. 2001;25(4):402-408.
30. Vandesompele J, De Preter K, Pattyn F, et al. Accurate normalization of real-time quantitative RT-PCR data by geometric averaging of multiple internal control genes. *Genome Biol*. 2002;3(7):1-12.
31. Wagner W, Roderburg C, Wein F, et al. Molecular and secretory profiles of human mesenchymal stromal cells and their abilities to maintain primitive hematopoietic progenitors. *Stem Cells*. 2007;25(10):2638-2647.
32. Alakel N, Jing D, Muller K, et al. Direct contact with mesenchymal stromal cells affects migratory behavior and gene expression profile of CD133+ hematopoietic stem cells during ex vivo expansion. *Exp Hematol*. 2009;37(4):504-513.
33. Villa A, Guerrini MM, Cassani B, et al. Infantile malignant, autosomal recessive osteopetrosis: the rich and the poor. *Calcif Tissue Int*. 2009;84(1):1-12.
34. Even-Or E, Stepensky P. How we approach malignant infantile osteopetrosis. *Pediatric Blood Cancer*. 2021;68(3):e28841.
35. Rieger K, Marinets O, Fietz T, et al. Mesenchymal stem cells remain of host origin even a long time after allogeneic peripheral blood stem cell or bone marrow transplantation. *Exp Hematol*. 2005;33(5):605-611.
36. Crane GM, Jeffery E, Morrison SJ. Adult haematopoietic stem cell niches. *Nat Rev Immunol*. 2017;17(9):573-590.
37. Szade K, Gulati GS, Chan CK, et al. Where hematopoietic stem cells live: the bone marrow niche. *Antioxid Redox Signal*. 2018;29(2):191-204.
38. Le PM, Andreeff M, Battula VL. Osteogenic niche in the regulation of normal hematopoiesis and leukemogenesis. *Haematologica* 2018;103(12):1945-1955.
39. Matsubara T, Kinbara M, Maeda T, et al. Regulation of osteoclast differentiation and actin ring formation by the cytolinker protein plectin. *Biochem Biophys Res Commun*. 2017;489(4):472-476.
40. Ferlin A, Pepe A, Facciolli A, et al. Relaxin stimulates osteoclast differentiation and activation. *Bone* 2010;46(2):504-513.
41. Chen W, Twaroski K, Eide C, et al. TCIRG1 transgenic rescue of osteoclast function using induced pluripotent stem cells derived from patients with infantile malignant autosomal recessive osteopetrosis. *JBJS* 2019;101(21):1939-1947.
42. Blin-Wakkach C, Wakkach A, Sexton P, et al. Hematological defects in the oc/oc mouse, a model of infantile malignant osteopetrosis. *Leukemia*. 2004;18(9):1505-1511.
43. Cheng H, Zheng Z, Cheng T. New paradigms on hematopoietic stem cell differentiation. *Protein Cell*. 2020;11(1):34-44.
44. Lu R, Czechowicz A, Seita J, et al. Clonal-level lineage commitment pathways of hematopoietic stem cells in vivo. *Proc Natl Acad Sci USA*. 2019;116(4):1447-1456.

45. Singh P, Mohammad KS, Pelus LM. CXCR4 expression in the bone marrow microenvironment is required for hematopoietic stem and progenitor cell maintenance and early hematopoietic regeneration after myeloablation. *Stem Cells*. 2020;38(7):849-859.
46. Cao H, Cao B, Heazlewood CK, et al. Osteopontin is an important regulative component of the fetal bone marrow hematopoietic stem cell niche. *Cells*. 2019;8(9):985.
47. Stegge M. *Interactions between hematopoietic stem cells and their niche*. 2020.
48. Tamma R, Ribatti D. Bone niches, hematopoietic stem cells, and vessel formation. *Int J Mol Sci*. 2017;18(1):151.
49. Lee D, Kim DW, Cho J-Y. Role of growth factors in hematopoietic stem cell niche *Cell Biol Toxicol*. 2020;36(2):131-144.
50. Zhao M, Tao F, Venkatraman A, et al. N-cadherin-expressing bone and marrow stromal progenitor cells maintain reserve hematopoietic stem cells. *Cell Rep*. 2019;26 (3):652-669. e656.
51. Li P, Zon LI. Resolving the controversy about N-cadherin and hematopoietic stem cells. *Cell Stem Cell*. 2010;6(3):199-202.